PALEOCEANOGRAPHY, VOL. 12, NO. 4, PAGES 533-545, AUGUST 1997

Modeled estimates of global reef habitat and carbonate production since the last glacial maximum

J. A. Kleypas

National Center for Atmospheric Research, Boulder, Colorado.

Abstract. Estimated changes in reef area and $CaCO_3$ production since the last glacial maximum (LGM) are presented for the first time, based on a model (ReefHab) which uses measured environmental data to predict global distribution of reef habitat. Suitable reef habitat is defined by temperature, salinity, nutrients, and the depth-attenuated level of photosynthetically available radiation (PAR). $CaCO_3$ production is calculated as a function of PAR. When minimum PAR levels were chosen to restrict reef growth to 30 m depth and less, modern reef area totaled 584–746 $\times$ 10^3 km^2. Global carbonate production, which takes into account topographic relief as a control on carbonate accumulation, was 1.00 $Gt\,yr^{-1}$. These values are close to the most widely accepted estimates of reef area and carbonate production and demonstrate that basic environmental data can be used to define reef habitat and calcification. To simulate reef habitat changes since the LGM, the model was run at 1-kyr intervals, using appropriate sea level and temperature values. These runs show that at the LGM, reef area was restricted to 20% of that today and carbonate production to 27%, due primarily to a reduction in available space at the lower sea level and secondarily to lower sea surface temperatures. Nonetheless, these values suggest that reef growth prior to shelf flooding was more extensive than previously thought. A crude estimate of reef-released CO_2 to the atmosphere since the LGM is of the same order of magnitude as the atmospheric CO_2 change recorded in the Vostok ice core, which emphasizes the role of neritic carbonates within the global carbon cycle. This model currently addresses only the major physical and chemical controls on reef carbonate production, but it provides a template for estimating shallow tropical carbonate production both in the present and in the past. As such, the model highlights several long-standing issues regarding reef carbonates, particularly in terms of better defining the roles of light, temperature, aragonite saturation state, and topography on reef calcification.

Introduction

Neritic carbonates have been a major sink for calcium carbonate and therefore are an important component of the global carbon cycle [*Milliman,* [1993]; *Milliman and Droxler,* 1996]. Carbonates produced in shallow tropical waters, in particular, are often preserved not only because of the high rates of deposition but also because a large portion is deposited above the lysocline. The magnitude of this sink has changed over time depending on factors such as temperature, sea level, continental distribution, and the predominant reef-building organisms (e.g., bivalves, sponges, corals, algae). *Milliman* [1993] estimated that roughly half of the $CaCO_3$ accumulated in the ocean basins today is stored as coral reefs, banks, and other neritic carbonates, but this figure was probably reduced during the last glacial maximum ((LGM) 21–18 ka), when sea level was below that of the continental shelves and reef growth was restricted to narrow zones along the steeper continental slopes.

The increase in $CaCO_3$ production on continental shelves relative to that in ocean basins during sea level rise is the basis for the "coral reef hypothesis," introduced by *Berger* [1982] and revisited by *Opdyke and Walker* [1992]. This hypothesis highlights coral reef carbonate production as one mechanism forcing Quaternary climate fluctuations. For every mole of marine $CaCO_3$ precipitated and preserved, approximately 0.6 mol of CO_2 is released to the atmosphere [*Ware et al.,* 1992; *Frankignoulle et al.,* 1994]. Although the present CO_2 increase due to reef calcification is only about 1% of that due to fossil fuel combustion [*Ware et al.,* 1992], neritic calcification is probably an important carbon cycle process over geologic time periods.

This paper presents the results of a new model for calculating $CaCO_3$ production in shallow tropical carbonate environments. This model, known as ReefHab, predicts reef habitat on the globe and accumulation of $CaCO_3$ within these habitats as a function of four major physical/chemical factors: temperature, salinity, nutrients, and light [*Kleypas,* 1995]. The model is also used to estimate changes in reef habitat area and $CaCO_3$ production since the LGM, based on global changes in sea level and sea surface temperature (SST).

Because ReefHab is designed for global studies, it is important to note two important features regarding its scale. First, the model is based on corals as the main carbonate producers within predicted reef habitats. Certainly, many other organisms contribute to carbonate production within a reef habitat. The most significant of these, the calcareous algae, have calcification rates similar to those of corals [*Bak,* 1976], and ReefHab does not distinguish their relative $CaCO_3$ production. Second, because of the coarse resolution of the model (~85 km^2), "reef" predictions tend to include two other tropical environments of carbonate deposition: submerged carbonate banks and *Halimeda* bioherms.

Although corals and other reef-building organisms occur over a wide range of environmental conditions, reefs de-

Paper number 97PA01134.
0883-8305/97/97PA-01134$12.00

velop only where calcium carbonate production exceeds its loss. Environmental conditions therefore control reef development in two ways: (1) directly, by limiting reef-building organisms, and (2) indirectly, by affecting net production of calcium carbonate.

In ReefHab, salinity, nutrients, and temperature all exert direct environmental control on reef distribution but not on reef calcification, while light is assumed to indirectly limit reef distribution by controlling calcification rate. Salinities which vary from 25 to 40 are reef-limiting [*Coles and Jokiel,* 1992], because unfavorable (usually lower) salinities directly exclude reef-builders rather than interfere with $CaCO_3$ production. Similarly, nitrate and phosphate are thought to directly control reef occurrence where elevated concentrations enhance the growth of noncalcareous algae, which compete with corals for space and light.

How temperature affects reef occurrence is less certain, even though it is an obvious environmental control on reef distribution. Reefs generally do not develop where minimum winter temperatures fall below 16°–18°C. However, the relative effects of direct (elimination of species) versus indirect (reduction of calcification) temperature constraints on reef development are not known. Defining how temperature affects reef occurrence is complicated by the positive correlation of temperature with daylight and with saturation state. Aragonite saturation state has received little attention but has recently been suggested as a potentially important factor in both coral and coralline algal growth [*Smith and Buddemeier,* 1992] and in carbonate accumulation [*Opdyke and Wilkinson,* 1993].

Finally, most reef-building organisms are light-limited, and hence they are confined to shallow, transparent waters which guarantee sufficient light penetration necessary for photosynthesis. In this case, reef development appears to be a function of photosynthetically available radiation ((PAR) wavelengths 400–700 nm) and its attenuation with depth. This is reflected in the general observation that coral extension rates decline logarithmically with depth (Figure 1). Even though individual corals present a wide range of calcification versus depth profiles, the most practical assumption for an entire reef community is that calcification is a linear function of photosynthesis. *Bosscher and Schlager* [1992] used this assumption to model vertical reef accumulation as a function of light and sea level change by replacing the photosynthesis versus irradiance (P-I) curve with a calcification versus irradiance curve (Figure 2). The hyperbolic tangent function used to calculate the curves in Figure 2 is most commonly used to represent the P-I relationship, although other equations have been derived to take into account photoadaptation [*Chalker and Marsh,* 1992].

Currently, there are few estimates of present-day coral reef area and no published estimates of reef area change since the LGM. Modern-day reef area estimates vary considerably (Table 1). The most often quoted and applied figure is 617 $\times$ 10^3 km^2 provided by *Smith* [1978], which he considered conservative.

Methods

Determination of Reef Habitat

The diagnostic model ReefHab (Figure 3) was used to determine potential habitats for reef growth based on global environmental data of salinity, sea surface temperature, nutrients, and light (as a function of solar irradiance incident on the sea surface, water depth, and water clarity; Table 2) [*Kleypas,* 1995]. All of the limiting values used to define reef habitat were initially determined from values quoted in the literature, although exact values presented in this paper were iteratively determined based on comparisons of model predictions with known reef locations. ReefHab predicts reef habitat at the same resolution as the topography data set (5′×5′) since water depth variations occur over small scales and have a strong control over reef distribution. Spatial resolution of the other input variables is much coarser (e.g., 1°×1° for salinity); however, these data do not vary considerably within their respective resolutions.

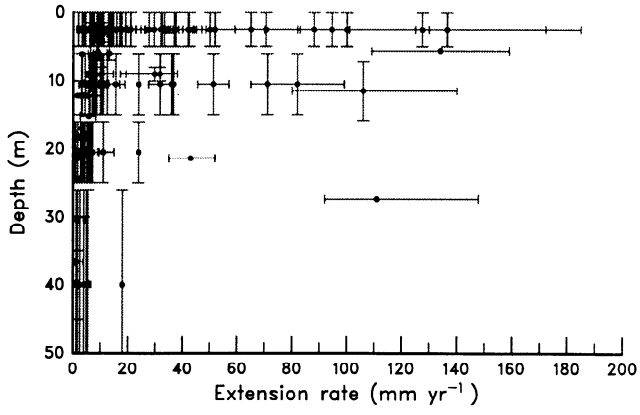

Figure 1. Plot of coral extension rates in millimeters per year versus depth. Most data are from original compilation by *Huston* [1985b], who grouped data into depth ranges 0–5 m, 6–15 m, 16–25 m, and > 25 m. Compilation is from a wide variety of sources and is displayed here to illustrate reduction in growth with depth across a wide variety of locations and species, and as originally stated by *Huston* [1985b, p. 21], "any application of statistical tests is of dubious validity." Additional sources are from *Hudson* [1981], *Wellington and Glynn* [1983], *Hubbard and Scaturo* [1985], *Tomascik and Sander* [1985], and *Guzmán and Cortés* [1989]. Outlier at 24 m depth is from *Tunnicliffe* [1983], recorded as average branch extension rate of three *Acropora* individuals.

Monthly salinity values for the global oceans were obtained from *Levitus* [1994]. These were used to directly limit reef habitat to regions where average monthly salinity remains between 30 and 39.

Nutrient concentrations (nitrate and phosphate) were obtained from *Levitus et al.* [1993]. In the absence of data on nutrient levels acceptable to reef development, the known global distribution of coral reefs was compared with the distribution of both nitrate and phosphate concentrations [*Kleypas,* 1995]. The best correlation of nutrient concentrations with reef distribution (as determined visually from global charts) occurred when annual average concentrations of surface nitrate remained below 2.0 μmol L^{-1} and phosphate remained below 0.20 μmol L^{-1}.

Sea surface temperature data were derived from 15 years of weekly satellite data combined with in situ measurements [*Reynolds and Marsico,* 1993]. Reefs were limited to where weekly sea surface temperatures remained between 18.1 and 31.5°C, except for enclosed seas, where reef habitat was allowed between 15.0° and 33.5°C.

Light was used to define reef habitat by first calculating the maximum depth of "adequate" light penetration at a

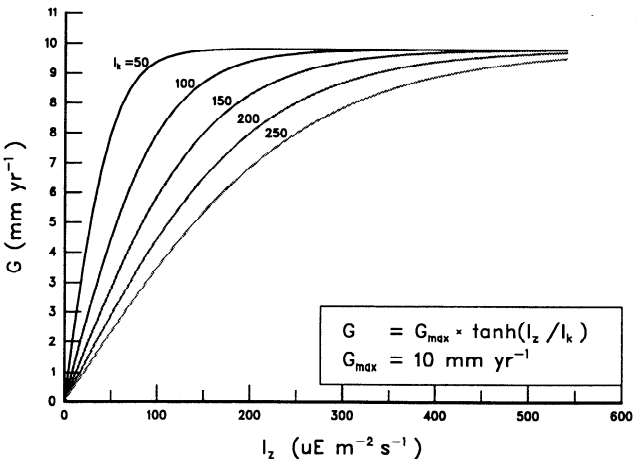

Figure 2. Calcification (expressed as vertical accumulation rate) versus irradiance curves for a typical hermatypic coral. G = vertical accumulation rate; I_z = photosynthetically active radiation (PAR) at depth z, in μE m^{-2} s^{-1}; I_k = PAR at the light compensation depth; and G_{max} = maximum possible vertical accumulation. Calcification is assumed to be a linear function of photosynthesis.

particular point and then testing whether the topographic point lies above or below that depth. The most comprehensive ocean topography data set available is ETOPO5 [*Sloss*, 1986], which has a spatial resolution of 5′ latitude and a depth resolution of 1 m. However, its accuracy is poor in waters shallower than 200 m, evidenced by spikes (mostly at 10-m intervals) in the hypsometric curve (Figure 4). These spikes are artifacts of how uncharted shelf waters were interpolated from surrounding waters (P. Sloss, personal communication, 1996). Errors in the ETOPO5 data set were treated by randomly redistributing excess values within a spike to within ±10 m of the spike.

The maximum depth of reef growth (z_{max}) was determined according to the equation

$$z_{max} = \frac{\log(I_{min}/\mathrm{PAR})}{K_{490}}$$

where I_{min} = minimum light intensity necessary for reef growth (μE (μEinsteins) m^{-2} s^{-1}); PAR = average daily PAR at sea surface (μE m^{-2} s^{-1}); and K_{490} = diffuse extinction coefficient of light of wavelength 490 nm (m^{-1}).

Estimated daily average PAR at the Earth's surface was obtained from *Pinker and Laszlo* [1992], who determined PAR at 2.5° × 2.5° resolution by combining a radiative transfer model with cloud cover data from the International Satellite Cloud Climatology Project (ISCCP). These PAR values thus reflect not only orbital and atmospheric changes but also cloud effects. The annual average PAR reaching the Earth's surface is fairly constant in the tropics but drops off rapidly at higher latitudes (Figure 5). In ReefHab calculations, average daily PAR was converted from W m^{-2} to μE m^{-2} s^{-1} by multiplying by a factor of 4.6 [*Kirk* 1994, p. 5]. Average PAR at the sea surface was attenuated with depth using the diffuse attenuation coefficient of light of wavelength 490 nm (K_{490}) derived from coastal zone color scanner (CZCS) data. The following conditions were assumed:

1. The K_{490} values were assumed to be valid in coastal waters, where most coral reefs exist. On the basis of comparisons of CZCS-derived K_{490} values with secchi disk depth data [*Kleypas*, 1995], this assumption is adequate for the broad applications of ReefHab.

2. The attenuation of wavelength 490 nm was assumed representative of that of the absorption spectra for zooxanthellae. *Falkowski et al.* [1990] report that zooxanthellae absorption occurs in a broad peak at 400–550 nm and in a narrower peak at 650–700 nm. Attenuation of wavelengths 650–700 nm (reds) is very high, but the average attenuation of wavelengths 400–550 nm (blues) is closely approximated by that of wavelength 490 nm. Since the 490-nm wavelength is most often the least attenuated in seawater, it closely represents the PAR wavelength of maximum penetration and hence the maximum depth at which zooxanthellae can photosynthesize.

Reef growth is obviously limited by some absolute light level, which explains their restriction to relatively shallow waters [*Huston*, 1985a]. Several researchers have subscribed to a general reef-limiting level of "10% of surface light," but this definition is confusing because surface light varies geographically. In ReefHab, a value of 10% of average surface PAR at the equator (50 μE m^{-2} s^{-1}) was first used as a limiting light level. The sensitivity of the model to this parameter was then tested by applying I_{min} values of 10, 25, 100, 150, 200, 250 and 300 μE m^{-2} s^{-1}.

Determination of Reef Carbonate Production

Vertical accumulation rate. Vertical accumulation rate was calculated according to the equation of *Bosscher and Schlager* [1992]:

$$G = G_{max}\tanh\frac{I_z}{I_k}$$

Table 1. Estimates of Area Extent of Present-Day Coral Reefs

Source	Estimate 10^3 km^2	Notes
Smith [1978]	617	reef coverage to 30 m depth
De Vooys [1979]	100	
Achituv and Dubinsky [1990]	2000	
Crossland et al. [1991]	617	used *Smith's* [1978] estimate to include photic zone reefs, where sediments are 80% reefal
Copper [1994]	1500	added relict reefs, carbonate banks, and interreef tract to *Crossland et al.* [1991] estimate
This study	584-3930	range of modeled results based on light-dependent reef depth limit

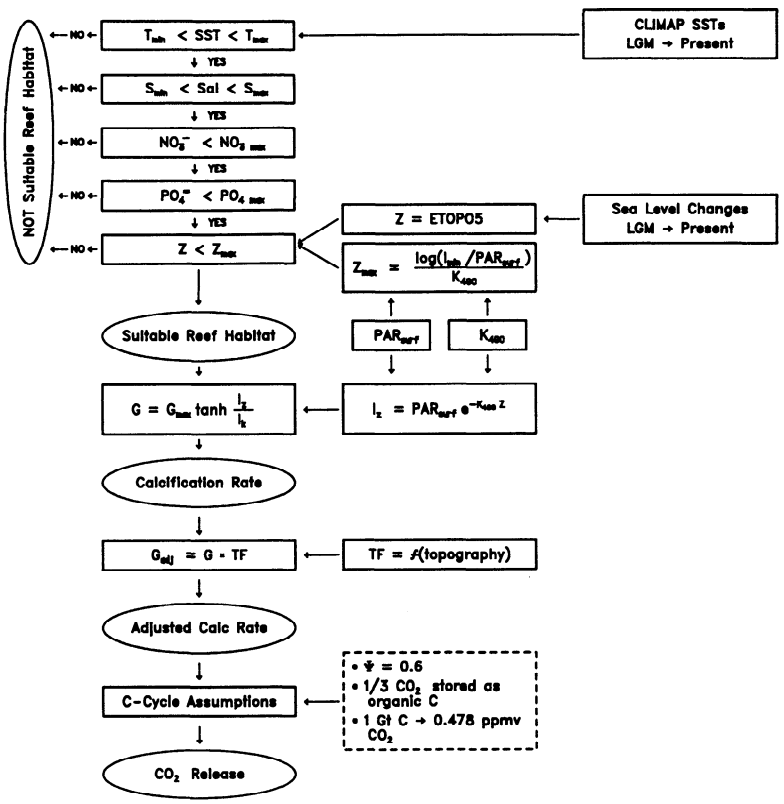

Figure 3. Generalized flow chart of ReefHab model inputs, calculations, and outputs. See text for details.

where

G vertical accumulation rate ($\mathrm{mm\,yr^{-1}}$);
$G_{\max}$ maximum vertical accumulation rate ($\mathrm{mm\,yr^{-1}}$);
I_z PAR at reef depth z ($\mu\mathrm{E\,m^{-2}\,s^{-1}}$) ($I_z = I_{\mathrm{surf}} e^{-K_{490} \cdot z}$);
I_k saturating light intensity necessary for photosynthesis ($\mu\mathrm{E\,m^{-2}\,s^{-1}}$).

A maximum vertical accumulation rate ($G_{\max}$) of 10 mm $\mathrm{yr^{-1}}$ was input into the model and was derived from maximum vertical accumulation rates determined from reef cores ($11\ \mathrm{mm\,yr^{-1}}$[*Stearn et al.*, 1977]; $12\ \mathrm{mm\,yr^{-1}}$[*Davies and Hopley*, 1983]; $10\ \mathrm{mm\,yr^{-1}}$[*Buddemeier and Hopley*, 1988]). However, in calculating average carbonate production for an entire grid cell, vertical accumulation rates were scaled down an order of magnitude. This is because a 5′×5′ grid cell (Figure 6a) may include many reef environments: reef front, reef crest, leeward reef, reef flats, and reef slopes, all of which have measured differences in vertical accumulation rates. A significant portion of most cells also consists of interreef areas which still accumulate carbonate but at a much lower rate than actively growing reefs. Average production across all coral reef environments has been estimated

Table 2. Spatial and Temporal Scales of Environmental Data Used in ReefHab Model

Parameter and Source	Scale		Limiting Criteria
	Spatial	Temporal	
Salinity *Levitus* [1994]	1 deg	monthly	minimum monthly > 30.0 maximum monthly < 39.0
Sea surface temperature, °C *Reynolds and Marsico* [1993]	1 deg	weekly	minimum weekly > 18.1° maximum weekly < 31.5°
Nutrients, μmol $\mathrm{L^{-1}}$ *Levitus et al.* [1993]	1 deg	monthly	annual average NO_3^- < 2.0 μmol $\mathrm{L^{-1}}$ annual average $PO_4^{\equiv}$ < 0.2 μmol $\mathrm{L^{-1}}$
Water depth, m *Sloss* [1986]	5 min	–	where water depth < $z_{\max}$ $z_{\max}$ = depth of average PAR saturation according to $[\log(I_{\min}/\mathrm{PAR})]/K_{490}$ where $I_{\min}$ = 50 – 300 $\mu\mathrm{E\,m^{-2}\,s^{-1}}$
PAR, W $\mathrm{m^{-2}}$ *Pinker and Laszlo* [1992]	2.5 deg	monthly	see above
Water transparency, K_{490} *Arnone et al.* [1992]	18 km	monthly	see above

Abbreviations are PAR, photosynthetically available radiation; CZCS, coastal zone color scanner.

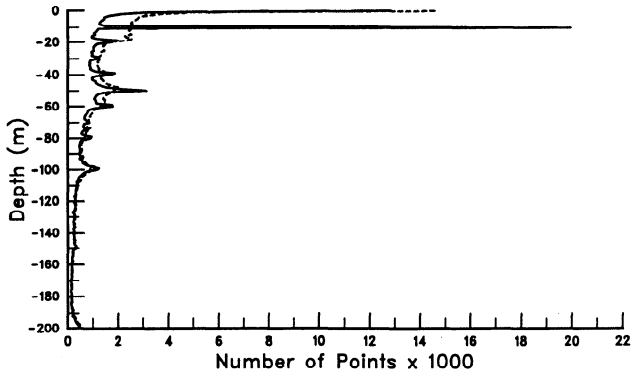

Figure 4. Distribution of water depths between 0 and 200 m, ETOPO5 database, 35°N–35°S. Dashed line shows distribution of water depths after excess values in spikes were randomly redistributed about ±10 m of the spike.

at 1200–1500 g $CaCO_3$ m^{-2} yr^{-1} [*Milliman,* 1993; *Milliman and Droxler,* 1996], which roughly equates to a vertical accumulation rate of 0.8–1.1 mm yr^{-1} (an order of magnitude lower than the maximum vertical accretion rates cited above). To calculate $CaCO_3$ production over an entire 5′×5′ grid cell, vertical accumulation rates (mm yr^{-1}) were converted to production (gigatons (Gt) yr^{-1}) using a conversion factor of 1.445 g cm^{-3} (this assumes a carbonate density of 2.89 g cm^{-3} and an average porosity of 50% [*Kinsey,* 1981]).

Values for I_k. I_k varies greatly between coral species, and I_k for an entire reef is a function of the reef community versus individual species. However, there are no established values of I_k for whole reefs. In terms of reef carbonate production rate, this value is more heavily weighted by the contribution of fast-growing frame-building corals. For example, vertical reef growth in the western Caribbean responded to sea level rise differently than that in the eastern Caribbean because two different species of *Acropora* dominate as frame-builders (*A. cervicornis* in the west and *A. palmata* in the east [*Macintyre,* 1972; 1988]). The saturating light intensity for *A. palmata,* an active framework coral in depths less than 5 m, is apparently higher than that of *A. cervicornis,* which builds framework down to 20 m depth. *Bosscher and Schlager* [1992] quoted I_k values of 50–450 $\mu E\, m^{-2}\, s^{-1}$ for a range of coral species and used values between 200 and 450 $\mu E\, m^{-2}\, s^{-1}$ in their light versus reef growth simulations without stipulating reasons for choosing these values.

Different light saturation intensities (I_k) between 50 and 300 $\mu E\, m^{-2}\, s^{-1}$ were used in separate model runs to calculate carbonate production rates. In each run, I_k was held constant on the globe, although undoubtedly there is variation in I_k across different coral communities. Calculated carbonate production for the southern Great Barrier Reef using an $I_k = 250$ $\mu E\, m^{-2}\, s^{-1}$ is shown in Figure 6b. It should be noted here that the above equation allows $CaCO_3$ production to depths greater than 30 m. That is, even though total reef area was restricted to depths 30 m and less, some vertical accumulation (about 20% using the above equation) does occur deeper than 30 m, and this is included in the estimates of total $CaCO_3$ production. This is evident in Figure 6 as vertical accumulation adjacent to but not directly within the confines of the well-defined reef.

Adjustment to carbonate production based on topography. A measure of topographic relief was devised to account for greater reef growth along topographic breaks and on topographic highs. The effects of topographic position on reef growth are obvious at several scales: Reefs tend to colonize topographic highs on otherwise flat shelves; reefs attain highest density on the edges of continental shelves and particularly on headlands; and reefs tend to grow faster where hydrographic exposure is high. *Bosence and Waltham* [1990] pointed to shelf architecture as a major control on carbonate platform development, and similarly parameterized shelf topography in their model, using distance from shoreline to adjust carbonate accumulation.

In ReefHab, a two-step process was used to parameterize topographic relief. First, topographic relief (α) at each 5′×5′ cell was derived by summing the slopes of the lines connecting a cell's centerpoint to the centerpoints of the surrounding eight cells, with downward slopes away from the point designated as positive and upward slopes as negative.

$$\alpha = \sum_{i=1}^{3}\sum_{j=1}^{3} \frac{\tan^{-1} Z_{i,j} - Z_{2,2}}{D_{i,j-2,2}}$$

where Z = grid cell depth (m); D = distance between grid cell centers (m); and i,j = row and column numbers of cells.

Thus α is a measure of overall relief of that location relative to the surrounding locations. Inner continental shelves tend to have little topographic relief (e.g., $\alpha = 0.1$); typical continental shelf breaks have moderate topographic relief (e.g., $\alpha = 1.7$); while atolls which rise steeply from the ocean floor have high topographic relief (α = 1.7–10.0; Figure 7). Since there is no evidence that atolls or reef areas near very steeply sloping continental shelves accumulate $CaCO_3$ more rapidly than shelf break reefs, values of α greater than 1.7 were reassigned to 1.7. Second, a topography factor (TF) of 0.05-1.00 was empirically derived using dynamic simulations of reef growth across a continental shelf in response to sea level rise (J. Kleypas, manuscript in preparation, 1997). These simulations were calibrated across several transects of the Great Barrier Reef, where actual Holocene reef thicknesses are well documented [e.g., *Hopley,* 1982; *Davies and Hopley,* 1983]. The following equation for TF yielded the most realistic reef thicknesses in the simulations.

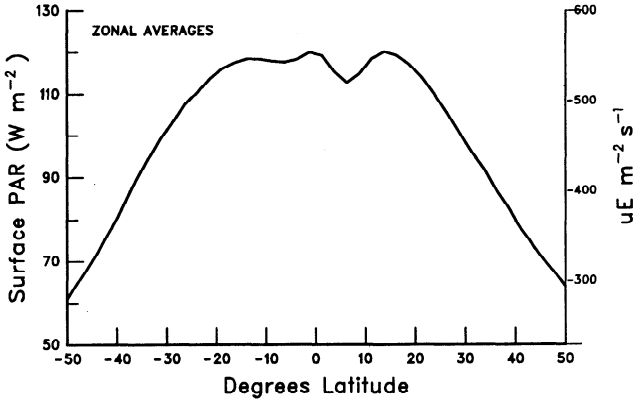

Figure 5. Zonally averaged PAR on the globe in both W m^{-2} and $\mu E\, m^{-2}\, s^{-1}$; data provided by *Pinker and Laszlo,* [1992]. The sharp dip in PAR at 5°N reflects increased cloudiness of the Intertropical Convergence Zone.

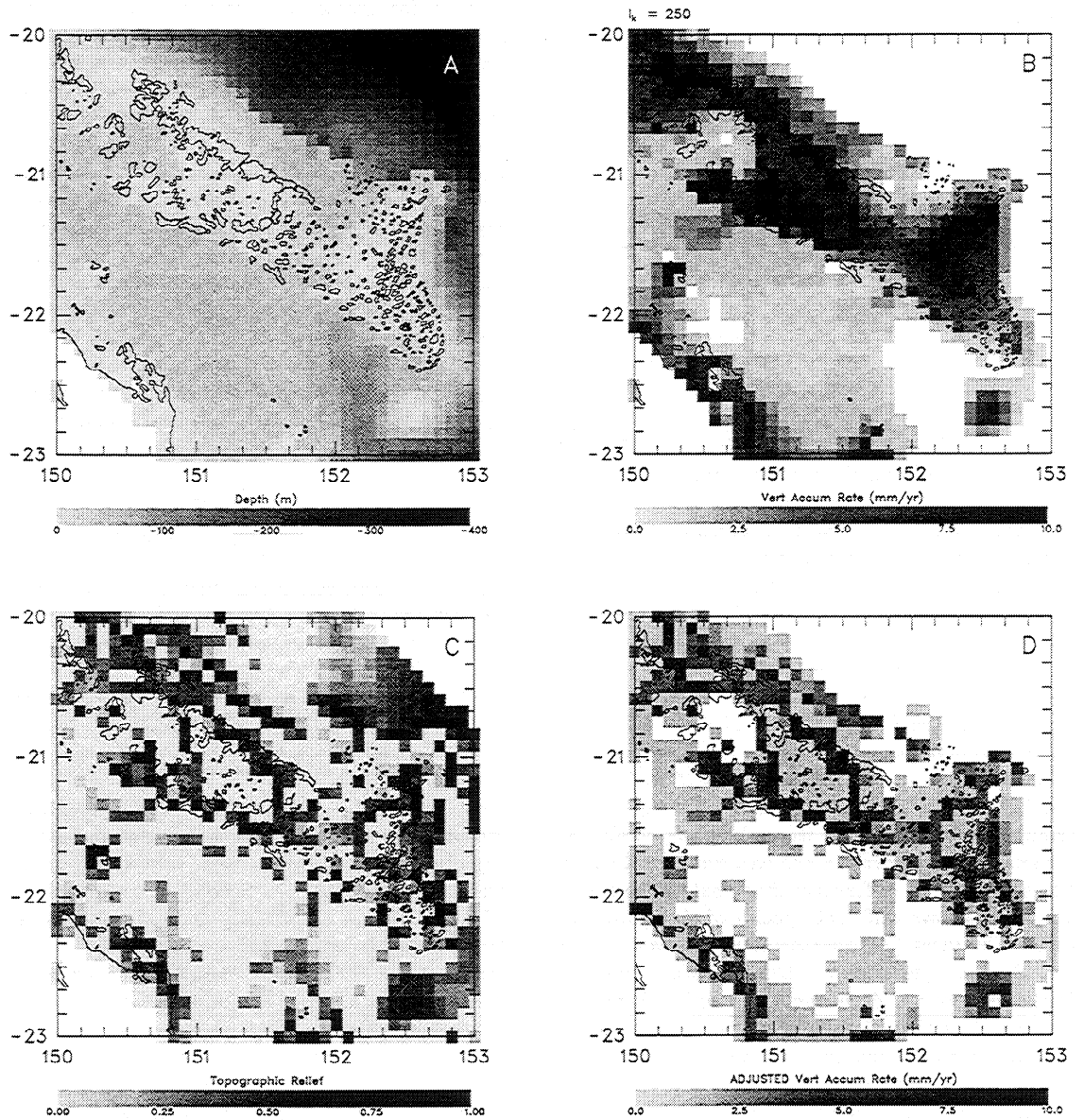

Figure 6. (a) $3° \times 3°$ section of the southern Great Barrier Reef, showing resolution of ETOPO5 $5' \times 5'$ topography. Coastline and reef outlines are overlain for comparison. This particular area comprises the Pompey and Swain Reefs. (b) Calculated vertical accumulation rates from ReefHab, using depths shown in Figure 6a, and average K_{490} values from coastal zone color scanner. $I_k = 250\ \mu\text{E}\,\text{m}^{-2}\,\text{s}^{-1}$. (c) Topography factor as parameterized from topographic relief. Low values indicate very little relief from surrounding locations, and high values indicate high relief. (d) Vertical accumulation rates, adjusted with topographic factor. Values are obtained by multiplying vertical accumulation values in Figure 6b by the topography factor in Figure 6c.

$$TF = \frac{\ln(\alpha \times 100)}{5}$$

The topography factor was used in the model to scale the vertical accumulation rate derived from the P-I curve (Figures 6c and 6d). For example, if the vertical accumulation rate at a particular location was determined to be 10 $\text{mm}\,\text{yr}^{-1}$ and the topography factor was 0.9, then the adjusted vertical accumulation rate was 9 $\text{mm}\,\text{yr}^{-1}$.

This factor provides a means of assessing the overall effects of topography on net accumulation, and factors affecting net accumulation (accretion, import/export, and dissolution) were not considered separately. Reefs along outer continental shelves and mid-ocean atolls have TFs near 1.0, so that maximum accumulation rates are observed, while topographically uniform inner continental shelves have TFs near 0.05, consistent with minimum accumulation rates observed for such regions.

Simulation of Changes in Reef Area and $CaCO_3$ Production Since the LGM

Changes in reef area cover and carbonate deposition since the LGM were calculated using ReefHab at 1-kyr intervals,

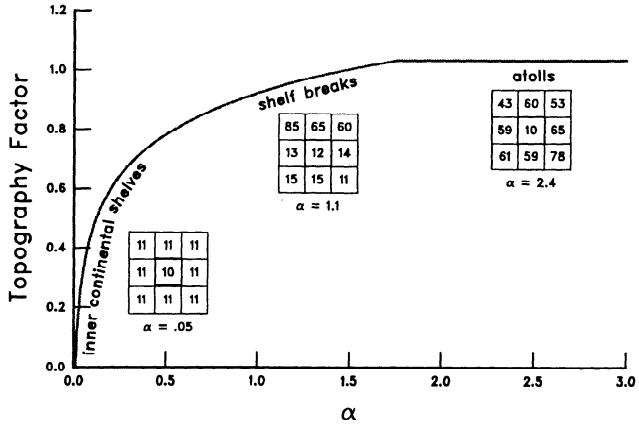

Figure 7. Relationship between α and topography factor. Typical 3×3 grids of water depth and resulting α values are illustrated for atolls, shelf breaks and inner continental shelves. Central grid cell is the value for which α is calculated, relative to the eight surrounding water depths.

using modifications of both sea level and SST. Sea level was adjusted according to the ice age paleotopography of *Peltier* [1994], which has a 1°×1° resolution and is compiled at 1-kyr intervals beginning with 21 ka.

The sensitivity of the model to temperature changes since the LGM was tested using three different SST scenarios: (1) assuming SSTs have been constant over the past 21 kyr (control); (2) using the CLIMAP Surface Configuration Data Base for 18 ka [*CLIMAP Project Members*, 1997] (CLIMAP); and (3) using two times the difference between CLIMAP and present-day values (CLIMAP×2). In scenarios 2 and 3, the 18-ka SST values were corrected to 21 ka based on the U-Th calibration of *Bard et al.* [1990], and the 21- to 0-ka SST curve was the same as that used in paleoclimate models [*Kutzbach and Ruddiman*, 1993; *Kutzbach et al.*, 1993]: The 21-ka SSTs were retained for the interval 21–18 ka, SST was linearly increased to present-day values between 18 and 6 ka, and present-day SSTs were used between 6 ka and the present. CLIMAP estimates of SSTs at the LGM are resolved at 2°×2° resolution. Tropical SSTs estimated in CLIMAP are considered conservative, on average being reported as only 1°–2°C cooler than those of today, while recent data indicate that tropical SSTs were around 3°–6°C cooler (see *Broecker* [1996] for a review and also *Bard et al.* [1997], *Beck et al.* [1997], *Curry and Oppo* [1997], and *Webb et al.* [1997]). True SSTs during the LGM were thus probably closer to the CLIMAP×2 simulations.

Light, water transparency, salinity, and nutrient concentrations were left unchanged in the simulations. On the basis of results of present-day model runs (Table 3), a minimum light level (I_{min}) of 250 $\mu E\,m^{-2}\,s^{-1}$ was used to determine reef area coverage. Total carbonate production was calculated using I_k = 250 $\mu E\,m^{-2}\,s^{-1}$.

Results

Estimates of Total Reef Area

ReefHab estimates of total reef area changed dramatically with the chosen light limit (Figure 8). Maximum depth of reef growth was reduced from 150 m to less than 30 m and total reef area from 3930 × 10^3 km^2 to 584 × 10^3 km^2, when I_{min} was increased from 10 to 300 $\mu E\,m^{-2}\,s^{-1}$ (Table 3). ETOPO5 hypsometry (Table 4) shows that more than 30% of tropical continental shelf areas (approximately the 0 to 200-m contour) is less than 30 m deep, compared with *Smith's* [1978] assumption that the 0 to 30 m interval (his depth limit for reefs) comprised only 15% of the 0 to 200-m contour. Still, Smith's reef area estimate of 617 × 10^3 km^2 is close to the model estimates when I_{min} = 250–300 $\mu E\,m^{-2}\,s^{-1}$ (746–584 × 10^3 km^2). These I_{min} values restrict reef growth in ReefHab to waters 30 m depth and less, but the choice of I_{min} depends on the definition of a coral reef. Lower values account for deeper-water reefs, which may be significant as diverse ecological communities but which probably contribute little to the global $CaCO_3$ budget,

The predicted distribution of reefs on the globe when I_{min} = 250–300 is similar to that of charted reef locations. Because not all coral reefs are charted on existing global maps,

Table 3. Reef Area Cover by Depth, Based on Different Reef-Limiting Light Levels

	I_{min}, $\mu E\,m^{-2}\,s^{-1}$							
Depth Range, m	10	25	50	100	150	200	250	300
0-9	568	568	563	508	457	411	362	313
10-19	1179	1122	747	662	63	475	381	271
20-29	333	305	253	151	73	24	3	< 1
30-39	302	266	206	77	16	1	< 1	
40-49	384	329	217	31	< 1			
50-59	428	330	131	2				
60-69	242	165	43					
70-79	181	91	5					
80-89	126	52	< 1					
90-99	100	12						
100-109	57	1						
110-119	20	< 1						
120-129	9							
130-139	2							
140-149	< 1							
TOTAL	3930	3242	2166	1432	1109	911	746	584

Except where noted, all values are × 10^3 km^2.

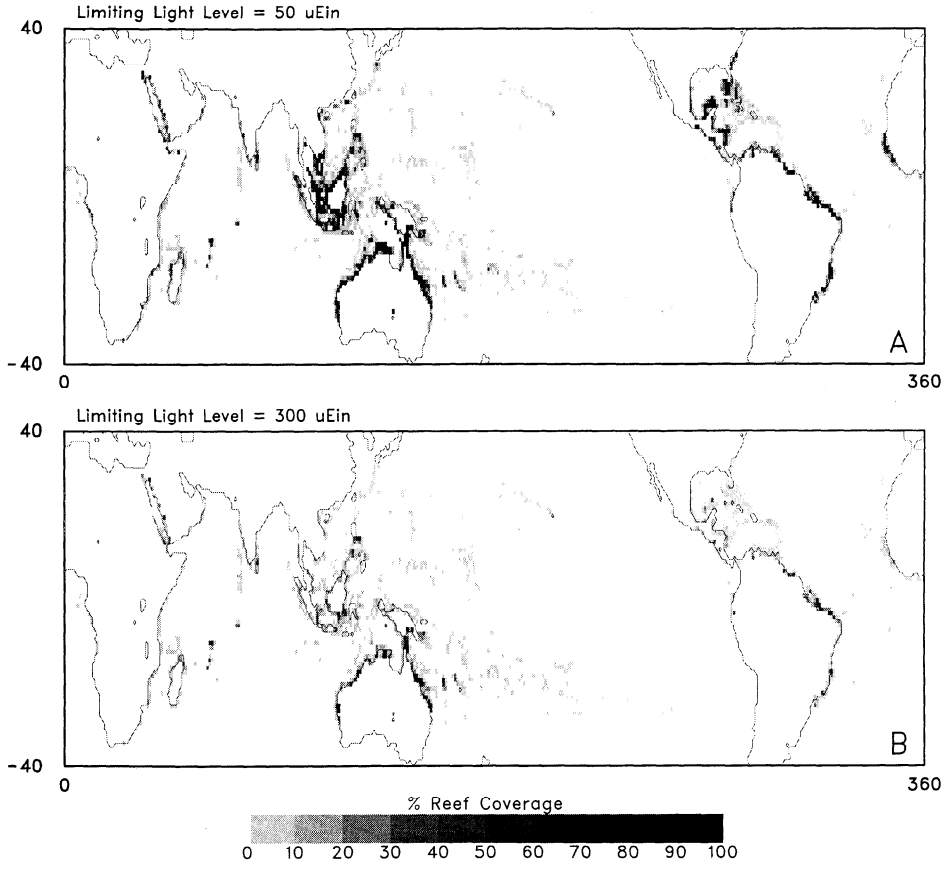

Figure 8. Predicted reef habitat as determined when reef-limiting PAR level is (a) 50 $\mu E\,m^{-2}\,s^{-1}$ and (b) 300 $\mu E\,m^{-2}\,s^{-1}$. For clarity, 5′ resolution results have been averaged to 1°; shading indicates the percentage of 5′×5′ cells within the 1° cell which are suitable reef habitat.

type I errors of the model (failure to predict a known reef location) are easier to verify than type II errors (false positive predictions). Type I errors are evident in the Arabian Sea and around the Spratly Islands (southeast of the Philippines), where the model fails to predict any reefs. Type II errors are most evident off eastern South America and western Africa, where reefs are overpredicted. Most type II errors can be traced to inaccuracies in the input data (e.g., annually averaged K_{490} values off South America do not adequately represent seasonally high turbidity during Amazon floods, and ETOPO5 topography of third world countries is often derived from poor-resolution charts). ReefHab appears to overpredict more often than underpredict reef habitat, but it apparently predicts locations of several previously uncharted submerged reefs in Indonesian waters (J. McManus, ICLARM, personal communication, 1996).

Present-Day $CaCO_3$ Deposition Rates

Present-day $CaCO_3$ rates were calculated at each cell in ReefHab and then summed to obtain a global figure. Three major points can be drawn from Figure 9, which illustrates calculated changes in carbonate production as a function of depth and different light saturation intensities, and Table 5, which shows total carbonate deposition in gigatons per year. First, the topography parameter reduced light-dependent carbonate production by a factor of 2.5–3.0. Second, total calculated carbonate production nearly doubled as light saturation intensity was reduced from 300 $\mu E\,m^{-2}\,s^{-1}$ to 50 $\mu E\,m^{-2}\,s^{-1}$. Third, the topography-adjusted values were reasonably close to *Milliman's* [1993] figure of 0.9 $Gt\,yr^{-1}$,

Table 4. Topographic Areas Within Depth Zones on the World's Continental Shelves Between 35°N and 35°S

Depth Range, m	Total Area, 10^3 km^2	Cumulative Area, 10^3 km^2	Cumulative Percent of 0–200 m Area
0-9	1,057	1,057	8.2
10-19	2,143	3,200	24.9
20-29	1,667	4,867	37.9
30-39	860	5,727	44.6
40-49	872	6,599	51.4
50-59	1,155	7,754	60.4
60-69	1,087	8,841	68.8
70-79	673	9,514	74.1
80-89	540	10,054	78.3
90-99	422	10,476	81.6
100-109	550	11,025	85.8
110-119	413	11,438	89.1
120-129	248	11,686	91.0
130-139	215	11,901	92.7
140-149	194	12,095	94.2
150-159	212	12,307	95.8
160-169	154	12,461	97.0
170-179	131	12,592	98.1
180-189	120	12,713	99.0
190-199	130	12,843	100.0

Data based on ETOPO5 world topography [*Sloss*, 1986], corrected to remove spikes.

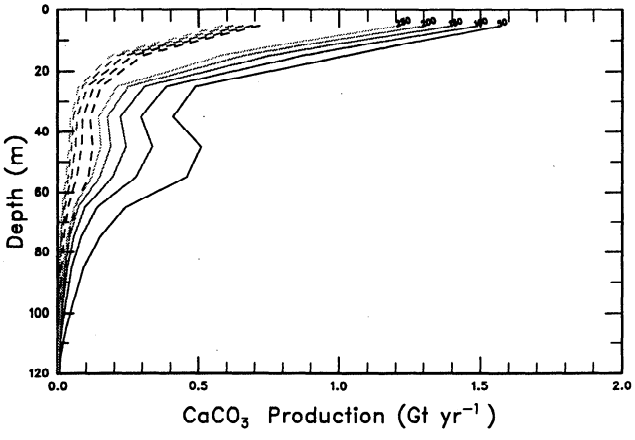

Figure 9. Carbonate production with depth, based on different light saturation intensities (I_k). Solid lines represent unadjusted carbonate production with I_k values indicated. Dashed lines represent carbonate production using the same I_k values but adjusted with the topography factor.

while unadjusted values were at least twice as high, even when I_k was as limiting as 300 $\mu E\,m^{-2}\,s^{-1}$.

Estimated Changes in Reef Area Cover and $CaCO_3$ Production Since the LGM

Modeled changes in reef area cover for the last 21 kyr, using an I_{min} = 250 $\mu E\,m^{-2}\,s^{-1}$ (which restricted reef growth to 30 m or less), showed that reef area increased rapidly as sea level rose and flooded the continental shelves, until 6 ka, after which reef area dropped slightly to present-day coverage (Figure 10a). Changes in reef $CaCO_3$ production rate reflected changes in reef area (Figure 10b). $CaCO_3$ production initially peaked at 11 ka, and then leveled out between 7 and 1 ka. Topographically adjusted production was less than one third that of unadjusted values. CLIMAP simulations reduced control values of reef area cover and $CaCO_3$ production at the LGM to 8 and 6%, respectively, and CLIMAP×2 simulations reduced controls by 12 and 13%.

Calculated changes in $CaCO_3$ production were compared to atmospheric CO_2 records since the LGM for evidence that reef growth might be reflected in atmospheric CO_2 changes. CO_2 concentration since the LGM as recorded in the Vostok ice core [*Barnola et al.*, 1987; *Barnola et al.*, 1991] increased as reef area and carbonate production increased (Figure 10), although the peak in atmospheric CO_2 concentration appears to predate the peak in reef carbonate production by about 2 kyr.

Atmospheric CO_2 concentration is the product of a wide variety of processes operating at different timescales [*Siegenthaler and Sarmiento* 1993]. Treatments of the effects of shelf versus basin carbonate deposition on atmospheric CO_2 are given by *Opdyke and Walker* [1992] and *Archer and Maier-Reimer* [1994]. Total production of CO_2 by ReefHab reef growth was grossly calculated using relationships established by previous researchers, with only broad consideration of the redistribution of that CO_2 once in the atmosphere. The primary relationship is that at pCO_2 = 350 μatm, Ψ = 0.6 (Ψ = moles CO_2 released : moles $CaCO_3$ precipitated) [*Ware et al.*, 1992], although *Frankignoulle et al.* [1994] showed that Ψ has increased from around 0.55 at the LGM to 0.67 today. Using Ψ = 0.6, for every gigaton of $CaCO_3$ precipitated (mol wt = 100), 0.072 Gt of C are available for release to the atmosphere (mol wt = 12 × 0.6). As much as a third of the CO_2 released may be taken up by organic C production, which if stored, would reduce this value to as low as 0.048 Gt of C [*Ware et al.*, 1992]. Finally, each gigaton of C added to the atmosphere as CO_2 corresponds to a CO_2 change of 0.478 ppmv (parts per million by volume) [*Houghton et al.*, 1994]. For example, the current rate of reef $CaCO_3$ production quoted by *Milliman and Droxler* [1996] of 0.9 Gt yr^{-1} theoretically releases 0.043 Gt C to the atmosphere each year, which corresponds to a 0.02 ppmv yr^{-1} change in atmospheric CO_2.

The reef contribution to atmospheric CO_2 since the LGM was thus calculated as a function of carbonate production over each 1-kyr period and was determined for topographically adjusted carbonate production only (Figure 10c). This crudely calculated flux of reef-produced CO_2 to the atmospheric (295 ppmv since LGM) is more than 3 times that reflected in the Vostok ice core (80 ppmv). As shown in Figure 10c, a two-thirds reduction of the calculated reef CO_2 production provides an approximate match for the Vostok CO_2 increase.

Discussion

Assessment of ReefHab

The more conservative ReefHab estimates of both reef area cover and $CaCO_3$ deposition are close to those obtained by other researchers. These values can be and have been calculated from existing knowledge of where and how deep reefs actually occur. However, such knowledge is incomplete, particularly for marginal environments where $CaCO_3$ is being deposited but which are not included in current estimates of reef coverage, and also for previous time periods for which reef area coverage is very poorly known. The values of the modeling approach presented here are thus (1) it potentially introduces less bias into estimates of reef coverage and $CaCO_3$ deposition because carbonate environments are assessed based on measured environmental factors and not on previously charted reef locations and (2) it allows extrapolation of reef carbonate production to other time periods.

However, as with any modeled versus real data, one must consider the model assumptions. The assumptions underlying the estimates of reef carbonate production presented in this paper are addressed below.

Table 5. Changes in Net Annual $CaCO_3$ Production Using Different Light Saturation Intensities

I_k, $\mu E\,m^{-2}\,s^{-1}$	Unadjusted $CaCO_3$ Production, Gt yr^{-1}	Adjusted $CaCO_3$ Production, Gt yr^{-1}
50	5.04	1.68
100	3.97	1.42
150	3.33	1.24
200	2.88	1.11
250	2.54	1.00
300	2.26	0.90

Adjusted $CaCO_3$ production was derived for each cell by multiplying unadjusted production by the topography factor.

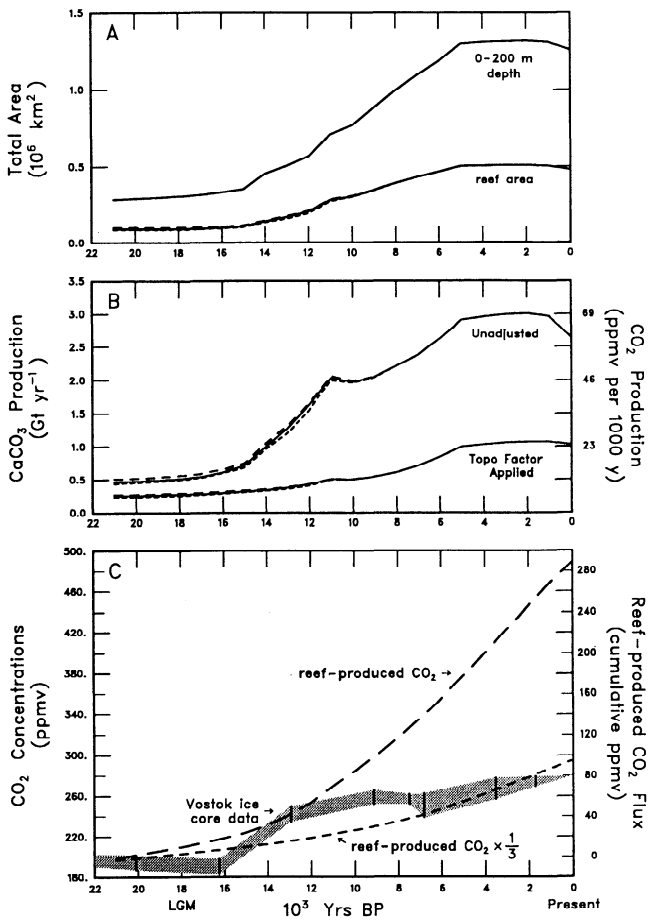

Figure 10. (a) Calculated changes in both total area between 0 and 200 m depth, and reef area, between LGM and present. Solid, dashed, and dotted lines illustrate sensitivity of model to SST: solid, model runs using CLIMAP SST values; dashed, runs using present day SST values; and dotted, runs using CLIMAP×2 values. (b) Calculated changes in total reef $CaCO_3$ production since LGM, using an I_k of 250 μE m^{-2} s^{-1}. Solid, dashed and dotted lines indicate same SST conditions as in Figure 10a. (c) Comparison of reef-released CO_2 to the atmosphere with concentrations preserved in the Vostok ice core [*Barnola et al.*, 1987, 1991]. Shaded area represents atmospheric CO_2 concentrations from the Vostok ice core; measurements are marked by vertical lines. Dashed lines represent cumulative increase in reef-released CO_2, calculated using adjusted reef carbonate production in Figure 10b, and again using one third that value.

Input data are adequately resolved and accurate. The major problems with ReefHab are the spatial resolution of some input data and reduced accuracy of ETOPO5 depths shallower than 200 m. As environmental data become better resolved, predictions of reef habitat and carbonate production rates will improve.

Calcification is a linear function of light intensity. Total calcification on a reef is the sum of calcification by its individual species; therefore each reef community should respond differently to the underwater light regime. ReefHab assumes these differences are minor from reef to reef. However, the different responses of eastern versus western Caribbean reefs to Holocene sea level change [*Macintyre*, 1988] demonstrate the need to consider how calcification versus irradiance varies between reef communities. An ideal method would be to apply known P-I curves of all constituent corals and other calcifying organisms on a given reef, but this would require unattainably detailed knowledge of the abundance, depth distribution, and calcification versus irradiance curves for all calcifying species of various reef communities.

The effects of other environmental factors on reef calcification (as opposed to reef distribution) are not yet considered in ReefHab. Temperature has often been suggested as a control on coral growth rates [*Gladfelter et al.*, 1978; *Grigg*, 1982, 1988; *Tomascik and Logan*, 1990], but this relationship has not been quantified separately from the effects of light or saturation state. Also at higher latitudes, seasonal differences may exert a strong influence on both the maximum depth of reef growth and on total calcification. In these regions, where maximum depth of light penetration can vary over several tens of meters, photosynthetically driven calcification may be more heavily augmented by heterotrophic feeding, in which case the assumption that calcification is linearly related to photosynthesis would not be valid.

Finally, net calcification on a reef must take into account not only precipitation of calcium carbonate but total loss as well. If carbonate losses are constant, then extrapolating reef accumulation from reef core data (as was done in deriving maximum accumulation rates) inherently includes these values. Even if such losses are not constant, as indicated by studies on bioerosion across different environments [*Hutchings*, 1986; *Hallock*, 1988; *Risk et al.*, 1995] and estimates of carbonate transport off reefs [*Hubbard et al.*, 1990], the factors controlling carbonate loss are still insufficiently defined to be modeled at the global scale.

Topography affects reef carbonate deposition. The topography factor was incorporated in the model in an attempt to localize reef calcification on the most exposed portions of continental shelves. Although there is no preexisting measure of how topography affects carbonate deposition rates, its parameterization in ReefHab appears to reflect actual deposition better than the assumption that topography has no effect. Therefore calculations of $CaCO_3$ production which incorporate the topography factor are considered more realistic.

Changes in Reef Area Cover and $CaCO_3$ Production Since the LGM

ReefHab calculations indicate that even if environments favorable to reef growth existed during and since the LGM, total area available was reduced to about 25–50% that of the present until flooding of continental shelves at 8–10 ka. Most of the reduction in reef growth was clearly due to lack of available space. In the LGM simulation, lowered sea level accounted for a reduction in reef area cover to 20% of present-day values and $CaCO_3$ production to 27%. By comparison, lower SSTs at the LGM, by reducing the latitudinal extent of reefs (recall that temperature was used as a control on reef distribution but not calcification), reduced reef area cover and $CaCO_3$ production only to 80–90% of controls. Only sea level and SST were changed in the ReefHab determination of reef growth since the LGM; although these are thought to be the most important factors limiting reef growth during this period, changes in the other variables surely imparted some effects on reef growth.

Two closely related variables that may have further reduced reef growth at times are turbidity and nutrients. For

example, water clarity was thought to have been so reduced during flooding of the insular shelves in the Caribbean that some reefs drowned when decreased light availability resulted in significant reduction of their calcification rates [*Adey et al.*, 1977; *Macintyre*, 1988; *Buddemeier and Hopley*, 1988]. In addition, growth of the Great Barrier Reef was suppressed for 1200–2000 years after initial shelf flooding, probably due to increased nutrient concentrations and/or turbidity [*Hopley*, 1994], while at the same time, *Halimeda* bioherm development was enhanced. (Note that in this case, because *Halimeda* calcification rates rival those of coral reefs [*Freile et al.*, 1995; *Hillis*, 1997], a reduction of coral $CaCO_3$ production does not necessarily mean a drop in total $CaCO_3$ production in reef habitats.)

Another variable thought to have affected reef growth is sea level surges. Some reef drownings or hiatuses in reef growth appear to have been caused by catastrophic surges in sea level rise associated with ice sheet collapse [*Chappell and Polach*, 1991; *Edwards et al.*, 1993; *Blanchon and Shaw*, 1995; *Larcombe et al.*, 1995; *Bard et al.*, 1996]. This version of ReefHab did not consider the rate of sea level rise to be a factor in overall reef calcification and assumed that whether as a constructional reef or as a thin veneer, reef calcification continued throughout sea level change through keep-up and catch-up strategies [*Neumann and Macintyre*, 1985] or backstepping [*Hubbard*, 1992].

ReefHab estimates of reef calcification since the LGM provide the basis for calculations of reef-contributed CO_2 flux to the atmosphere. Comparison of Figures 10b and 10c suggests that the sharp increase in atmospheric CO_2 concentration at 13 ka preceded the peak in $CaCO_3$ production by 2 kyr. Indeed, ice core chronology indicates that most of the global warming and sea level rise since the LGM lagged atmospheric CO_2 increase by 2–3 kyr [*Sowers and Bender*, 1995]. It thus seems more logical that increased reef growth is a consequence rather than a cause of the atmospheric CO_2 increase. However, in positive feedback, increased reef growth since the LGM likely contributed to the atmospheric CO_2 reservoir.

Crude estimates of CO_2 production by these reefs are of the same order of magnitude as atmospheric CO_2 concentrations recorded in the Vostok ice core. However, these values represent a one-way flux into the atmospheric CO_2 reservoir only, and do not reflect subsequent adjustments by the many interrelated feedback mechanisms (e.g., biospheric and oceanic uptake and dissolution of shelf carbonates during lowered sea level). Present-day measurements indicate that about a third of the anthropogenic releases of CO_2 is absorbed by the oceans [*Siegenthaler and Sarmiento*, 1993], and over the timescale of millenia, deep-ocean circulation should further lower atmospheric CO_2 levels through dissolution of carbonates near the carbonate compensation depth. These processes may help explain the two-thirds reduction needed to bring the given estimate to within the range recorded in the Vostok ice core (Figure 10c).

A better measure of the magnitude of this flux might be to compare total shallow shelf carbonate deposition rates obtained from ReefHab with rates used in the *Opdyke and Walker* [1992] model designed to test the coral reef hypothesis. ReefHab $CaCO_3$ production increased from 0.26 Gt yr^{-1} at the LGM to a maximum of 1.07 Gt yr^{-1} at 2 ka, while the *Opdyke and Walker* model fluctuated total shelf $CaCO_3$ sedimentation between -0.7 and 2.3 Gt yr^{-1} (dissolution of exposed shelf carbonates during lower sea level accounts for the negative lower limit). Their higher estimates were sufficient to explain atmospheric CO_2 fluctuations to within a few ppmv, so it is reasonable to say that according to their model, ReefHab carbonate deposition rates are too low to explain the Vostok ice core results alone. However, the magnitude of the reef-produced CO_2 fluxes is not inconsistent with the estimates of total carbonate effects.

Kayanne [1992] disputed the coral reef hypothesis based on geologic cross sections of several shelf reefs which became established at 7–8 ka. However, because of the lack of geologic data from off-shelf reefs, this approach naturally neglects reef growth prior to 8 ka. Continued discovery of submerged and drowned reefs in the tropics worldwide indicates that coral reef development in waters off the edges of continental and insular shelves prior to shelf transgression was more extensive than formerly thought [*Macintyre*, 1972; *Hine and Steinmetz*, 1984; *Moore and Fornari*, 1984; *Harris and Davies*, 1989; *Moore et al.*, 1990; *Vora and Almeida*, 1990; *Ludwig et al.*, 1991; *Lidz et al.*, 1991; *Macintyre et al.*, 1991; *Rougerie et al.*, 1992]. There is also recent evidence that a mass mortality event on a reef may be succeeded by extremely rapid rates of erosion [*Eakin*, 1996; *Glynn*, 1997]. Hence evidence for such reefs may be lacking in the geologic record, and indeed, ReefHab does not take into account such calcification losses.

Conclusions

This paper represents the first attempt to use environmental variables to analyze and predict modern reef distribution and to quantify changes in reef habitat and calcification since the LGM. ReefHab results indicate that (1) within limits defined by temperature, nutrients and salinity, the latitudinal and depth distribution of PAR (photosynthetically available radiation) and the benthic area available can satisfactorily predict many aspects of modern reef distribution; (2) unless environmental requirements for coral reef development were significantly reduced during the last marine transgression, reef growth prior to shelf flooding was probably more extensive than previously thought; and (3) the role of neritic carbonates, and reefs in particular, in the global carbonate budget is potentially quite important and should be more closely examined.

This research contributes to and emphasizes the importance of several long-standing issues regarding coral reef growth: (1) At what level of detail and with what accuracy can reef calcification be regarded as a function of PAR and its attenuation with depth? (2) How does temperature affect coral and reef calcification rates? (3) What is the effect of aragonite saturation state on coral and reef calcification? (4) How does submarine topography influence reef calcification and carbonate accumulation? (5) What geologic evidence of early Holocene reef growth do we have?

Acknowledgments. The author thanks the Advanced Study Program and Starley Thompson at the National Center for Atmospheric Research for financial and logistical support to conduct this research. Jon Bergengren of the Climate Change Research Section of NCAR encouraged this project from the start, and Steve Worley of the Data Support Section assisted with acquisition of many of the data

sets. Rachel Pinker of the University of Maryland kindly provided the PAR data sets. Conversations with John McManus and Terry Done were quite helpful during the model design and applications. Special thanks are reserved for Bob Buddemeier, who obviously spent a long time editing an early version of the manuscript. Many thanks also to Clive Wilkinson, Peter Glynn, and an anonymous reviewer, whose comments are greatly appreciated.

References

Achituv, Y., and Z. Dubinsky, Evolution and zoogeography of coral reefs, in *Ecosystems of the World, vol. 25, Coral Reefs,* edited by Z. Dubinsky, chap. 1, pp. 1-9, Elsevier, New York, 1990.

Adey, W. H., I. G. Macintyre, and R. Stuckenrath, Relict barrier reef system off St. Croix: Its implications with respect to late Cenozoic coral reef development in the western Atlantic, *Proc. Int. Coral Reef Symp., 3rd,* 2, 15-21, 1977.

Archer, D., and E. Maier-Reimer, Effect of deep-sea sedimentary calcite preservation on atmospheric CO_2 concentration, *Nature, 367,* 260-263, 1994.

Arnone, R. A., G. Terrie, L. Estep, and R. A. Oriol, Ocean optical database, *Tech. Note 254,* Naval Oceanogr. and Atmos. Res. Lab., Stennis Space Cent., Miss., 42 pp, 1992.

Bak, R. P. M., The growth of coral colonies and the importance of crustose coralline algae and burrowing sponges in relation to carbonate accumulation, *Neth. J. Sea Res., 10,* 285-337, 1976.

Bard, E., B. Hamelin, R. G. Fairbanks, and A. Zindler, Calibrations of the ^{14}C timescale over the past 30,000 years using mass spectrometric U-Th ages from Barbados corals, *Nature, 345,* 405-410, 1990.

Bard, E., B. Hamelin, M. Arnold, L. Montaggioni, G. Cabioch, G. Faure, and F. Rougerie, Deglacial sea-level record from Tahiti corals and the timing of global meltwater discharge, *Nature, 382,* 241-244, 1996.

Bard, E., F. Rostek, and C. Sonzogni, Interhemispheric synchrony of the last deglaciation inferred from alkenone paleothermometry, *Nature, 385,* 707-710, 1997.

Barnola, J. M., D. Raynaud, Y. S. Korotkevich, and C. Lorius, Vostok ice core profiles 160,000-year record of atmospheric CO_2, *Nature, 329,* 408-414, 1987.

Barnola, J. M., P. Pimienta, D. Raynaud, and Y. S. Korotkevich, CO_2-climate relationship as deduced from the Vostok ice core: A re-examination based on new measurements and on re-evaluation of the air dating, *Tellus, Ser. B, 43,* 83-90, 1991.

Beck, J. W., J. Récy, F. Taylor, R. L. Edwards, and G. Cabioch, Abrupt changes in early Holocene tropical sea surface temperature derived from coral records, *Nature, 385,* 705-707, 1997.

Berger, W. H., Increase of carbon dioxide in the atmosphere during deglaciation: The coral reef hypothesis, *Naturwissenschaften, 69,* 87-88, 1982.

Blanchon, P., and J. Shaw, Reef drowning during the last deglaciation: Evidence for catastrophic sea-level rise and ice-sheet collapse, *Geology, 23,* 4-8, 1995.

Bosence, D., and D. Waltham, Computer modeling the internal architecture of carbonate platforms, *Geology, 18,* 26-57, 1990.

Bosscher, H., and W. Schlager, Computer simulation of reef growth, *Sedimentology, 39,* 503-512, 1992.

Broecker, W., Glacial climate in the tropics, *Science, 272,* 1902-1904, 1996.

Buddemeier, R. W., and D. Hopley, Turn-ons and turn-offs: Causes and mechanisms of the initiation and termination of coral reef growth, *Proc. Int. Coral Reef Symp., 6th,* 1, 253-261, 1988.

Buddemeier, R. W., and S. R. Smith, Coral reef growth in an era of rapidly rising sea level: Predictions and suggestions for long-term research, *Coral Reefs, 7,* 51-56, 1988.

Chalker, B. E., and L. M. Marsh, Modeling primary production by reef-building corals: Functions that accommodate photoadaptation, *Proc. Int. Coral Reef Symp., 7th,* 1, 362 (abstract), 1992.

Chappell, J., and H. Polach, Post-glacial sea-level rise from a coral record at Huon Peninsula, Papua New Guinea, *Nature, 349,* 147-149, 1991.

CLIMAP Project Members, Seasonal reconstruction of the Earth's surface at the Last Glacial Maximum, *Geol. Soc. Am., Map Chart Ser.,* in press, 1997.

Coles, S. L., and P. L. Jokiel, Effects of salinity on coral reefs, in *Pollution in Tropical Aquatic Systems,* edited by D. W. Connell and D. W. Hawker, pp. 147-166, CRC Press, Boca Raton, Fla., 1992.

Copper, P., Ancient reef ecosystem expansion and collapse, *Coral Reefs, 13,* 3-11, 1994.

Crossland, C. J., B. G. Hatcher, and S. V. Smith, Role of coral reefs in global ocean production, *Coral Reefs, 10,* 55-64, 1991.

Curry, W. B., and D. W. Oppo, Synchronous, high-frequency oscillations in tropical sea surface temperatures and North Atlantic Deep Water production during the last glacial cycle, *Paleoceanography, 12,* 1-14, 1997.

Davies, P. J., and D. Hopley, Growth fabrics and growth rates of Holocene reefs in the Great Barrier Reef, *BMR J. Aust. Geol. Geophys., 8,* 237-251, 1983.

De Vooys, C. G. N., Primary production in aquatic environments, in *The Global Carbon Cycle,* edited by B. Bolin et al., pp. 259-292, John Wiley, New York, 1979.

Eakin, C. M., Where have all the carbonates gone? A model comparison of calcium carbonate budgets before and after the 1982-1983 El Niño at Uva Island in the eastern Pacific, *Coral Reefs, 15,* 109-119, 1996.

Edwards, R. L., J. W. Beck, G. S. Burr, D. J. Donahue, J. M. A. Chappell, A. L. Bloom, E. R. M. Druffel, and F. W. Taylor, A large drop in atmospheric $^{14}C/^{12}C$ and reduced melting in the Younger Dryas, documented with ^{230}Th ages of corals, *Science, 260,* 962-968, 1993.

Falkowski, P. G., P. L. Jokiel and R. A. Kinzie, III, Irradiance and corals, in *Ecosystems of the World, vol. 25, Coral Reefs,* edited by Z. Dubinsky, chap. 5, pp. 89-107, Elsevier, New York, 1990.

Frankignoulle, M., C. Canon, and J.-P. Gattuso, Marine calcification as a source of carbon dioxide: Positive feedback of increasing atmospheric CO_2, *Limnol. Oceanogr., 39,* 458-462, 1994.

Freile, D., J. D. Milliman, and L. Hillis, Leeward bank margin *Halimeda* meadows and draperies and their sedimentary importance on the western Great Bahama Bank slope, *Coral Reefs, 14,* 27-33, 1995.

Gladfelter, E. H., R. K. Monahan, and W. B. Gladfelter, Growth rates of five reef-building corals in the northeastern Caribbean, *Bull. Mar. Sci., 28,* 728-734, 1978.

Glynn, P. W., Eastern Pacific reef coral biogeography and faunal flux: Durham's dilemma revisited, *Proc. Int. Coral Reef Symp., 8th,* in press, 1996.

Grigg, R. W., Darwin Point: A threshold for atoll formation, *Coral Reefs, 1,* 29-34, 1982.

Grigg, R. W., Paleoceanography of coral reefs in the Hawaiian-Emperor Chain, *Science, 240,* 1737-1743, 1988.

Guzmán, H. M., and J. Cortés, Growth rates of eight species of scleractinian corals in the eastern Pacific (Costa Rica), *Bull. Mar. Sci., 44,* 1186-1194, 1989.

Hallock, P., The role of nutrient availability in bioerosion: Consequences to carbonate buildups, *Palaeogeogr. Palaeoclimatol. Palaeoecol., 63,* 275-291, 1988.

Harris, P. T., and P. J. Davies, Submerged reefs and terraces on the shelf edge of the Great Barrier Reef, Australia: Morphology, occurrence and implications for reef evolution, *Coral Reefs, 8,* 97-98, 1989.

Hillis, L., Importance of calcareous green algae to tropical reefs, *Proc. Int. Coral Reef Symp., 8th,* in press, 1996.

Hine, A. C., and J. C. Steinmetz, Cay Sal Bank, Bahamas – A partially drowned carbonate platform, *Mar. Geol., 59,* 135-164, 1984.

Hopley, D., *The Geomorphology of the Great Barrier Reef: Quaternary Development of Coral Reefs,* 453 pp., Wiley-Interscience, New York, 1982.

Hopley, D., Continental shelf reef systems, in *Coastal Evolution, Late Quaternary Shoreline Morphodynamics,* edited by R. W. G. Carter and C. D. Woodroffe, chap. 8, pp. 303-340, Cambridge Univ. Press, New York, 1994.

Houghton, J. T., L. G. Meira Filho, J. Bruce, H. Lee, B. A. Callander, E. Hartis, N. Harris, and K. Muskell, *IPCC: Radiative Forcing of Climate Change and an Evaluation of the IPCC IS92 Emission Scenarios,* Cambridge Univ. Press, New York, 1994.

Hubbard, D. K., A modern example of reef backstepping from the eastern St. Croix shelf, U. S. Virgin Islands, in *AAPG SEPM Annual Meeting Abstracts,* 57, Am. Assoc. Pet. Geol., Tulsa, Okla., 1992.

Hubbard, D. K., and D. Scaturo, Growth rates of seven species of scleractinian corals from Cane Bay and Salt River, St. Croix, USVI, *Bull. Mar. Sci., 36,* 325-338, 1985.

Hubbard, D. K., A. I. Miller, and D. Scaturo, Production and cycling of calcium carbonate in a shelf-edge reef system (St. Croix, U.S. Virgin Islands): Applications to the nature of reef systems in the fossil record, *J. Sediment. Petrol., 60,* 335-360, 1990.

Hudson, J. H., Growth rates in *Montastrea annularis*: A record of environmental change in Key Largo Coral Reef Marine Sanctuary, Florida, *Bull. Mar. Sci., 31,* 444-459, 1981.

Huston, M. A., Patterns of species diversity on coral reefs, *Annu. Rev. Ecol. Syst., 16,* 149-177, 1985a.

Huston, M. A., Variation in coral growth rates with depth at Discovery Bay, Jamaica, *Coral Reefs, 4,* 19-25, 1985b.

Hutchings, P. A., Biological destruction of coral reefs. A review, *Coral Reefs, 4,* 239-252, 1986.

Kayanne, H., Deposition of calcium carbonate into Holocene reefs and its relation to sea-level rise and atmospheric CO_2, *Proc. Int. Coral Reef Symp., 7th,* 1, 50-55, 1992.

Kinsey, D. W., The Pacific/Atlantic reef growth controversy, *Proc. Int. Coral Reef Symp., 4th,* 1, 493-498, 1981.

Kirk, J. T. O., *Light and Photosynthesis in Aquatic Ecosystems,* 2nd ed., 509 pp., Cambridge Univ. Press, New York, 1994.

Kleypas, J. A., A diagnostic model for predicting global coral reef distribution, in *Recent Advances in Marine Science and Technology '94,* edited by O. Bellwood et al., pp. 211-220, PACON Int. and James Cook Univ. of N. Queensland, Townsville, Australia, 1995.

Kutzbach, J. E., and W. F. Ruddiman, Model description, external forcing, and surface boundary conditions, in *Global Climates Since the Last Glacial Maximum,* edited by H. E. Wright Jr. et al., chap. 3, pp. 12-23, Univ. of Minn. Press, Minneapolis, 1993.

Kutzbach, J. E., P. J. Bartlein, I. C. Prentice, W. F. Ruddiman, F. A. Street-Perrott, T. Webb III, and H. E. Wright, Jr., Epilogue, in *Global Climates Since the Last Glacial Maximum,* edited by H. E. Wright Jr. et al., chap. 20, pp. 536-542, Univ. of Minn. Press, Minneapolis, 1993.

Larcombe, L., R. M. Carter, J. Dye, M. K. Gagan, and D. P. Johnson, New evidence for episodic post-glacial sea-level rise, central Great Barrier Reef, Australia, *Mar. Geol., 127,* 1-44, 1995.

Levitus, S., Climatological atlas of the world ocean, *NOAA Prof. Pap. 13,* 173 pp., U.S. Govt. Print. Off., Washington, D. C., 1994.

Levitus, S., M. E. Conkright, J. L. Reid, R. G. Najjar, and A. Mantyla, Distribution of nitrate, phosphate and silicate in the world oceans, *Prog. Oceanogr., 31,* 245-273, 1993.

Lidz, B. H., A. C. Hine, E. A. Shinn, and J. L. Kindinger, Multiple outer-reef tracts along the south Florida bank margin: Outlier reefs, a new windward-margin model, *Geology, 19,* 115-118, 1991.

Ludwig, K. R., B. J. Szabo, J. G. Moore, and K. R. Simmons, Crustal subsidence rate off Hawaii determined from $^{234}U/^{235}U$ ages of drowned coral reefs, *Geology, 19,* 171-174, 1991.

Macintyre, I. G., Submerged reefs of eastern Caribbean, *AAPG Bull., 56,* 720-738, 1972.

Macintyre, I. G., Modern coral reefs of the western Atlantic: New geological perspective, *AAPG Bull., 72,* 1360-1369, 1988.

Macintyre, I. G., K. Rutzler, J. N. Norris, K. P. Smith, S. D. Cairns, K. E. Bucher, and R. S. Stenick, An early Holocene reef in the western Atlantic: Submersible investigations of a deep relict reef off the west coast of Barbados, W. I., *Coral Reefs, 10,* 167-174, 1991.

Milliman, J. D., Production and accumulation of calcium carbonate in the ocean: Budget of a nonsteady state, *Global Biogeochem. Cycles, 7,* 927-957, 1993.

Milliman, J. D., and A. W. Droxler, Neritic and pelagic carbonate sedimentation in the marine environment: Ignorance is not bliss, *Geol. Rundsch., 85,* 495-511, 1996.

Moore, J. G., and D. J. Fornari, Drowned reefs as indicators of the rate of subsidence of the island of Hawaii, *J. Geol., 92,* 752-759, 1984.

Moore, J. G., W. R. Normark, and B. J. Szabo, Reef growth and volcanism on the submarine southwest rift zone of Mauna Loa, Hawaii, *Bull. Volcanol., 52,* 375-380, 1990.

Neumann, A. C., and I. Macintyre, Reef response to sea level rise: Keep-up, catch-up or give-up, *Proc. Int. Coral Reef Symp., 5th,* 3, 105-110, 1985.

Opdyke, B. N., and J. C. G. Walker, Return of the coral reef hypothesis: Basin to shelf partitioning of $CaCO_3$ and its effect on atmospheric CO_2, *Geology, 20,* 733-736, 1992.

Opdyke, B. N., and B. H. Wilkinson, Carbonate mineral saturation state and cratonic limestone accumulation, *Am. J. Sci., 293,* 217-234, 1993.

Peltier, W. R., Ice age paleotopography, *Science, 265,* 195-201, 1994.

Pinker, R. T., and I. Laszlo, Global distribution of photosynthetically active radiation as observed from satellites, *J. Clim., 5,* 56-65, 1992.

Reynolds, R. W., and D. C. Marsico, An improved real-time global sea surface temperature analysis, *J. Clim., 6,* 768-774, 1993.

Risk, M. J., P. W. Sammarco, and E. N. Edinger, Bioerosion in *Acropora* across the continental shelf of the Great Barrier Reef, *Coral Reefs, 14,* 79-86, 1995.

Rougerie, F., B. Wauthy, and J. Rancher, Le récif barrière ennoyé des Iles Marquises et l'effet d'île par endo-upwelling, *C. R. Acad. Sci., Ser. II, 315,* 677-682, 1992.

Siegenthaler, U., and J. L. Sarmiento, Atmospheric carbon dioxide and the ocean, *Nature, 365,* 119-125, 1993.

Sloss, P. W., Relief of the surface of the Earth. Tape formats for ETOPO5 minute gridded world elevations, data announcement, Mar. Geol. and Geophys. Div., Nat. Geophys. Data Cent., Boulder, Colo., 1986.

Smith, S. V., Coral-reef area and the contributions of reefs to processes and resources of the world's oceans, *Nature, 273,* 225-226, 1978.

Smith, S. V., and R. W. Buddemeier, Global change and coral reef ecosystems, *Annu. Rev. Ecol. Syst., 23,* 89-118, 1992.

Sowers, T., and M. Bender, Climate records covering the last deglaciation, *Science, 269,* 210-214, 1995.

Stearn, C. W., T. P. Scoffin, and W. Martindale, Calcium carbonate budget of a fringing reef on the west coast of Barbados, I, Zonation and productivity, *Bull. Mar. Sci., 27,* 479-510, 1977.

Tomascik, T., and A. Logan, A comparison of peripheral growth rates in the recent solitary coral *Scolymia cubensis* (Milne-Edwards and Haime) from Barbados and Bermuda, *Bull. Mar. Sci., 46,* 799-806, 1990.

Tomascik, T., and F. Sander, Effects of eutrophication on reef-building corals, I, Growth rate of the reef-building coral *Montastrea annularis, Mar. Biol., 87,* 143-155, 1985.

Tunnicliffe, V., Caribbean staghorn coral populations: Pre-Hurricane Allen conditions in Discovery Bay, Jamaica, *Bull. Mar. Sci., 33,* 132-151, 1983.

Vora K. H., and F. Almeida, Submerged reef systems on the central western continental shelf of India, *Mar. Geol., 91,* 255-262, 1990.

Ware, J. R., S. V. Smith, and M. L. Reaka-Kudla, Coral reefs: Sources or sinks of atmospheric CO_2?, *Coral Reefs, 11,* 127-130, 1992.

Webb, R. S., D. H. Rind, S. J. Lehman, R. J. Healy, and D. Sigman, Influence of ocean heat transport on the climate of the last glacial maximum, *Nature, 385,* 695-699, 1997.

Wellington, G. M., and P. W. Glynn, Environmental influences on skeletal banding in eastern Pacific (Panama) corals, *Coral Reefs, 1,* 215-222, 1983.

J. A. Kleypas, Climate Change Research Section, National Center for Atmospheric Research, P. O. Box 3000, Boulder, Colorado 80307. (e-mail: kleypas@ncar.ucar.edu)

(Received July 24, 1996; revised March 31, 1997;
accepted April 18, 1997.)